Journal of Information Science and Technology
JIST Journal of Information Science and Technology
Volume 13, NO 2 | JUL – DEC 2023 | 62-68
ISSN: 2651-1053 (Online)
ISSN: 1906-9553 (Print)

Design and Simulation of Chessboard Coding Wave Artifacts

*Tanatorn Tantipiriyakul and Komsan Kanjanasit**
College of Computing, Prince of Songkla University, Phuket Campus, 83120, Thailand

Received: November 2, 2023; Revised: December 18, 2023; Accepted: December 20, 2023; Published: December 29, 2023

ABSTRACT – This paper presents a numerical simulation of a binary chessboard-coding artifact in the designs of wave objects for upcoming smart communication in a centimeter-wave range. The binary-coding artificial structures can be composed of a mixture of two types of unit cells with the digital states of "0" and "1" elements in a two-dimensional (2D) structure. The binary characters are essential to a unity magnitude of a reflection type with the dependence of an opposite phase response at 0° and 180°. The proposed binary coding configuration relies on utilizing an artificial magnetic conductor (AMC) which is formed by a patch-based array over a perfect ground surface with a dielectric slab. The scattering characteristic is illustrated at the operating frequency of 10 GHz. The antenna device as a wave object is designed using the binary chessboard-coding artifact with a function of wave radiation. With a simulation technique, numerical analysis provides an understanding of the electromagnetic (EM) effect of binary-coding unit cells and antenna designs. The results of a computational process can identify the potential properties of the chessboard-coding artifact.

KEYWORDS: Chessboard Coding Artifact, Coding Metamaterial, Chessboard Metamaterial, Wave Object

1. Introduction

A new class of artificial structures has been proposed in the name of digital and coding metamaterials [1][2]. The coding metamaterial is fundamentally related to information metamaterial [3] and software-defined metamaterial [4]. The design concept can be connected between the digital signal domain and electromagnetic field (EMF) wave. These advanced metamaterials are highlighted by interfacing with a digital binary sequence for programmability and reconfigurability. The structural artifacts have been formed by applying non-uniform unit cells in a difference of phase and amplitude in a periodic platform. The discrete configurations are realized on the combination of two-type unit cells with an opposite reflection phase. The concept of information entropy can be used to explain the metamaterial mechanism [5]. The principle of generalized Snell's law describes the effect on the scattering angles of wave incidence by creating a mixture of discrete unit cells in phase-varied patterns [6]. The essence of metamaterial is also detailed to illustrate anomalous wave phenomena [7]. Modern methodology of machine learning techniques is applied to design physically unusual patterns to generate coding sequences on metamaterials [8]. The coding metamaterial comes with a phase and amplitude discontinuity to manipulate unusual wavefronts in radiation and serve as intelligent metasurfaces [9].

The designs of the reduction of radar cross-section (RCS) have been subjected to research works based on employing chessboard-coding metamaterials which have the potential to improve the scattering effect [10][11][12]. The metasurface is designed with a discontinuity of properties of periodic surfaces that is proposed to enhance antenna performance [13]. In addition, antenna objects can cooperate with chessboard periodic surfaces that have been introduced to enhance radiation characteristics [14]. The radiation mechanism relied on Fabry-Perot antennas in designing a superstrate, however, the configuration came up with a volumetric structure [15][16]. The chessboard supercell structures are complicated in terms of physical design. In this work, we emphasize the design of a planar chessboard-coding artificial structure. The antenna object is proposed as a wave artifact in the use of compact chessboard-coding patterns. The characterization of binary coding artificial structures is performed using a numerical simulation. The

*Corresponding Author: komsan.k@psu.ac.th

performance analysis and investigation are reflected to understand the EM effect of the scattering properties. As applied for a wave object, the antenna configuration is synthesized for a new-type planar artificial structure. The platform of a binary coding artifact and 2D synthesized antenna structure are demonstrated in Section 2. The numerical results and discussion of unit-cell and antenna objects are described in Section 3. The conclusion is detailed in Section 4.

2. Proposed Configurations

This section describes the configurations of the binary coding artifacts and the planar antennas in terms of design methodology and modeling.

2.1 The Chessboard-Coding Wave Object

The EM foundation of perfect electric and magnetic conductors is the essence of the duality of electromagnetism with distinct reflection-type phases. The concept behind chessboard-coding object design involves combining two reflective surfaces, comprising perfect electric conductor (PEC) and artificial magnetic conductor (AMC) structures. The PEC surfaces naturally exhibit a reflective phase of 180° due to their inherent conductivity. While the perfect magnetic conductor (PMC) material is unavailable in nature, AMC structures can be engineered using periodic resonators, offering a reflective phase of 0° in a particular frequency. These PEC and AMC structures exhibit electric and magnetic responses, symbolized as binary states to "1" and "0" elements. In this context, the chessboard coding wave artifact is created by the mixture of PEC and AMC units for wave manipulation with an internal field excitation in the planar structure as shown in Figure 1.

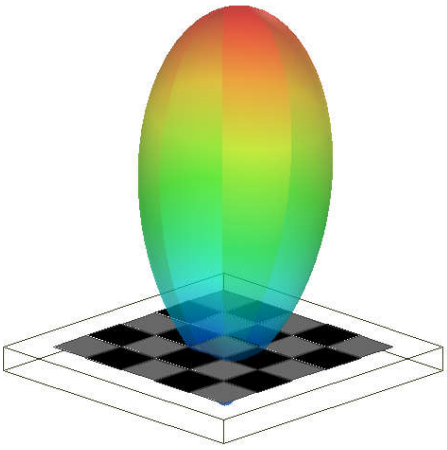

Figure 1. 3D view of the two-state chessboard-coding wave artificial object with a radiation pattern.

2.2 The Binary Coding Artifact Structure

Figure 2 shows the evolution of the binary-coding patterns of a supercell (a group of unit cells) to build an artificial structure using two types of basic capacitive unit cells. The fully and partially square metallic patches act as "1" (PEC) elements and "0" (AMC) elements to shape a double-side configuration. These configurations are used for designing a binary coding artifact. The periodic array of 2×2 cells of the binary patches is positioned on the top surface, whereas the blank metal is placed on the bottom surface of a dielectric slab. In this study, the dielectric property is a constant of 4.4 with zero loss tangent. These structural configurations are referred to as high-impedance surfaces. The AMC-based structure can be theoretically represented by a thin cavity with a phase-difference analysis [17]. The EM properties of a reflection and transmission-type phase are a fundamental element in investigating these binary coding supercells. The evolution of the supercells is created in different four patterns starting with the fully "0" uniform elements (Figure 2(a)), the vertical stripe (Figure 2(b)), the horizontal stripe (Figure 2(c)), and the chessboard (Figure 2(d)). It is illustrated that the chessboard can correspond to the bitwise operator utilizing the logic operator with an exclusive OR/NOR function between the vertical stripe and horizontal stripe.

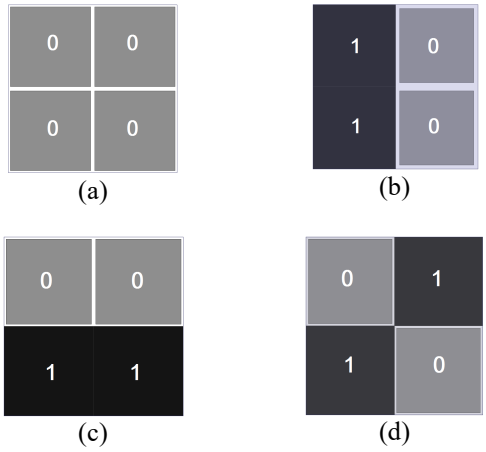

Figure 2. Schematic patterns of the evolution of the binary supercells from (a) toward (d) consisting of "0" and "1" elements in patterns of a) fully "0" uniform elements (uniform version), b) the vertical stripe, c) the horizontal stripe, and d) the chessboard patterns.

2.3 The Supercell Modeling

To analyze wave properties, the 2D periodic structure model is established based on an EM boundary condition. It enables the characterization of the field response of the designed unit cells. Figure 3 provides a depiction of the 3D structure, which is a supercell composed of the chessboard scheme. The analysis process can be applied using two structural models of the supercells. First, a pack of four binary-coding patch

elements with a ground surface is modeled referring to a high-impedance surface as shown in Figure 3(a). Second, a resonant cavity model is applied for the identical two-layer structure of four binary-coding patch elements as shown in Figure 3(b). Both models are performed in an environmental box with an infinity array equivalence. The boundary condition is based on Floquet's theory [18] to assign the setup of the PEC and PMC properties at a couple of the side faces of the modeled box. Therefore, the structural modeling of a binary coding artifact is created under an infinitive boundary condition. The two faces on the top and bottom are assigned by a wave-port function to excite EM energy. For a high-impedance surface in Figure 3(a), only one PORT is defined to obtain a reflection-type phase. In that, a unit reflection is achieved due to a metal-backed surface at the existing interface (no transmission). For a resonant cavity model in Figure 3(b), the field excitation is from PORT1 to PORT2 in obtaining a transmission response.

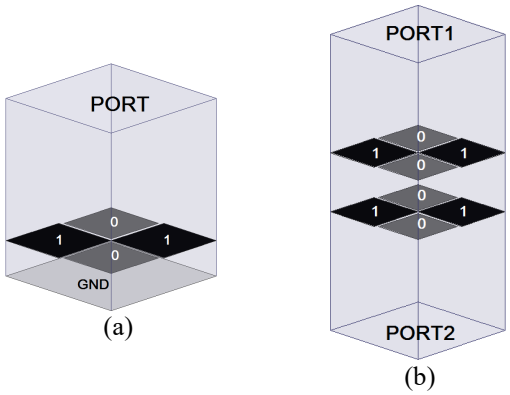

Figure 3. Unit-cell modeling of the binary coding artifact consists of a) the high-impedance surface, and b) the resonant cavity model.

2.4 The Antenna Object Configuration

To build a wave object, the two types of antenna design using a chessboard supercell are packed as a planar structure. Figure 4 shows the top-view layout of the interfacial surface patterned by periodic chessboard-coding cells. It consists of the Type-1 and Type-2 pattern designs which are inverted by cell elements for each other. In this study, the symmetric periodic array is also considered to form an antenna aperture with a 5×5 array dimension. The total 2D periodic cells are 25 elements. It is seen that the Type-1 and Type-2 designs consist of fully and partially metallic patches (PEC "1" / AMC "0") of 13/12 and 12/13 elements, respectively. The specific feature of the two designs is to highlight the impact of the center tile in the array surface that becomes the "0" and "1" elements.

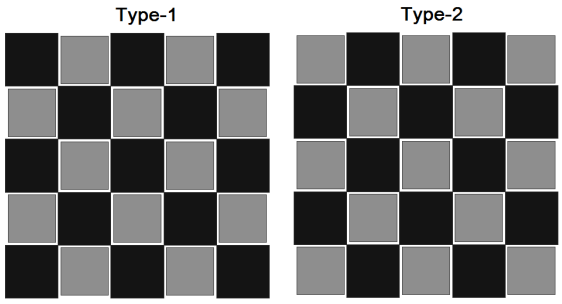

Figure 4. Periodic patterns of the 5×5 binary cells consisting of the Type-1 and the Type-2 (inverted Type-1) patterns.

Table 1. Physical dimensions in Figure 5 of a narrow aperture, CPW feeder, and patch array, in millimeters (mm).

Ls	Ws	Wf	G	P	L	H
14	0.5	20	0.1	3.9	3.7	2.0

The all-designed parameters of the antenna object are optimized and listed in Table 1. Figure 5 shows the schematic layout of the planar antenna object. Figure 5(a) shows the geometry in a top view of the primary field feeder on the bottom surface. The ground surface of the chessboard structure is mechanically slotted to include a driven field feeder and the wave signal port. Based on [19], the driven feeder is a narrow aperture element with the designed parameters of the length (Ls) = 14 mm and the width (Ws) = 0.5 mm. The Ls parameter is theoretically calculated using one wavelength at 10 GHz, whereas the width Ws is estimated at one-tenth dimension in the first design steps. In [20], the primary design of the parameters of the short-end CPW feeder based on 50–Ω characteristic impedance has the feedline width (Wf) = 20 mm and gap (G) = 0.1 mm, leading a wave signal to the narrow aperture. Figure 5(b) exhibits the schematic layout in a cross-section view of the periodic array surface on the top surface. The planar structure of the dielectric slab (dielectric constant = 4.4 and loss tangent = 0.025) is sandwiched by a primary feeder and the 5×5 chessboard-patterned surface. The design parameters of the square patch-based chessboard pattern are linked to the analysis of the supercell configuration in the previous section. In [21], the array period (P) = 3.9 mm and the patch length (L) = 3.7 mm are associated with a patch antenna theory and frequency selective surface. In that, the two types of unit cells are considered as a binary "0" element (partial patch is L = 3.7 mm and P = 3.9 mm) and as a binary "1" element (full patch is L = P = 3.9 mm). The total planar structure is 25 × 25 mm^2 (~0.5λ × ~0.5λ).

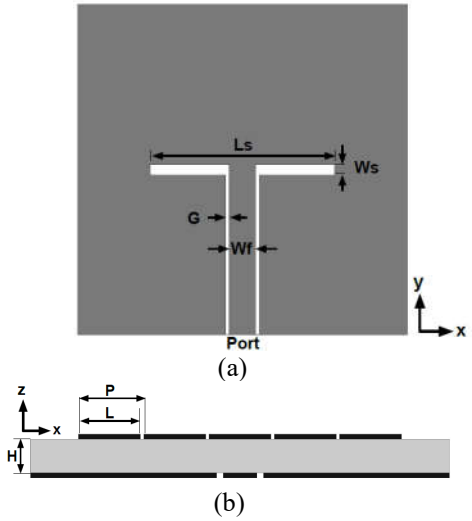

Figure 5. Antenna geometry: a) the bottom view of the feeder configuration using a narrow aperture with a CPW feeder as a magnetic dipole, and b) the side view of a double-side structure consisting of the feeder (bottom) and patch array surface (top).

3. Results and Discussion

This section reports the EM characterization of the binary coding artifacts and the planar antennas carried out using a numerical analysis. The full-wave simulation is performed to illustrate the potential properties of the resonance effect and RF characteristics.

3.1 The Supercell Characteristics

Based on a unit-cell simulation, the supercell can be characterized between the frequency range of 6 GHz and 14 GHz using a finite element method (FEM). The resonance effect comes with the EM interference of the periodic surface structure. To evaluate the stripe patterns, the resonance effect is around 10 GHz with the phase characteristic of reflection depicting a resonance condition by pole and zero. The peak and dip scheme of transmission represents the resonance characteristic. Figure 6 shows the line plots of reflection-phase responses for four study cases of the supercells. The distinct responses relate to a material characterization that comes with the electric and magnetic properties in two types of PEC and AMC elements, respectively. The full "0" supercell (four elements of a uniform patch-based AMC structure) as a baseline exhibits the resonance condition (reflection phase = 0°) at 6.9 GHz. Two versions of the stripe arrangement are investigated in vertical and horizontal patterns. The mixture of four elements of the fully and partially metallic patches illustrates a different resonance condition. For the vertical stripe pattern, the AMC resonance occurs at 10.4 GHz shifting by 3.5 GHz from a baseline response. In the case of the horizontal stripe pattern, the pole and zero phase responses are shown at 9.7 GHz and 10.3 GHz, respectively. In that, the AMC resonance conditions are close frequencies between two versions of stripe patterns. The supercell with the mixture of a chessboard pattern is unique by generating two resonant frequencies at 9.2 GHz and 13.4 GHz. It can be considered as a combination of the two effects of the strip patterns with shifting frequencies.

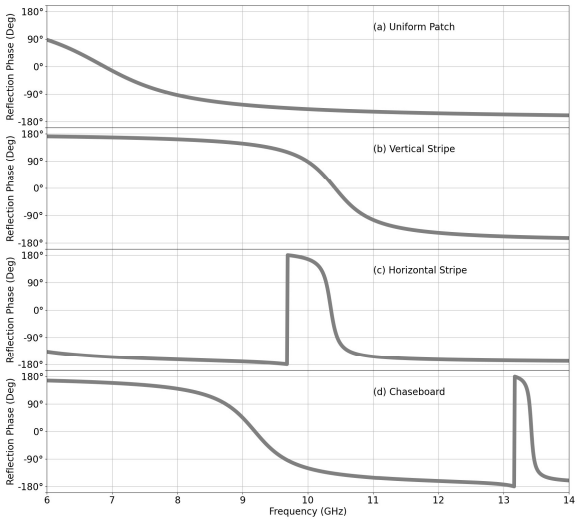

Figure 6. Response of reflection phases of the high-impedance surface model depicting a supercell evolution in Figure 2 from (a) to (d).

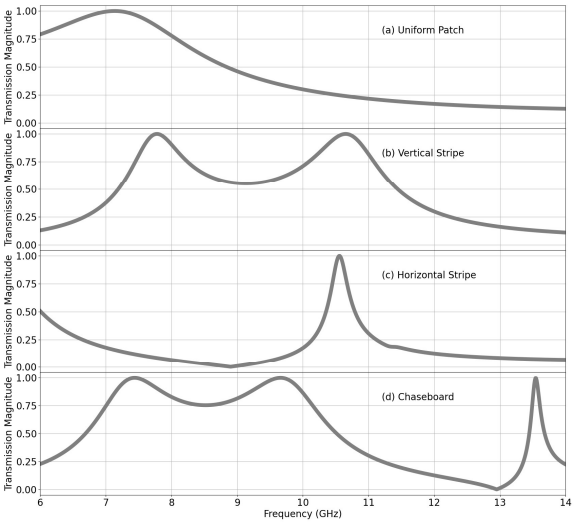

Figure 7. Response of transmission magnitude of the resonant cavity model depicting a supercell evolution in Figure 2 from (a) to (d).

With the resonant cavity model, the transmission properties are characterized to reveal the resonance effect in the chessboard-coding metamaterial. Figure 7 shows the line plots of the transmission responses for four study cases of the supercells. With responses to reflection phases, the transmission peaks arise to provide a resonant cavity with electric and magnetic

properties at the same frequencies. To understand the transmission response (peak and dip), only uniform-patch supercell provides a single resonance, whereas other binary-cell mixture cases give multiple resonances with different types. The baseline of the case of the full "0" four-element supercell presents the single peak. The vertical stripe pattern depicts an asymmetric profile of dip and peak according to pole and zero phases. The horizontal stripe pattern exhibits double transmission peaks with respect to the electric and magnetic resonance (referring to a 180° and 0° reflection phase response), respectively. In particular, the chessboard pattern reveals the collection of two attributes of double-peak and asymmetric-profile resonances with frequency shifting.

3.2 The Antenna Characteristics

The synthesized planar antenna is characterized to depict EM properties. The 3D configuration of the planar antenna structure using the chessboard-coding artifact is practically simulated in a radiation box as an environment setup. The impedance and reflection are investigated to obtain the high-performance attributes of impedance and radiation. Two numerical approaches are performed to analyze performance characteristics using a finite element method (FEM) and finite-difference time-domain (FDTD) approach. Figure 8 shows the impedance characteristic in real and imaginary components of the two design cases using chessboard alignment with a frequency range between 8.0 GHz and 12.00 GHz. The key responses are at the same operating frequency at 9.5 GHz. It illustrates that Type-1 provides a double-tune matching to obtain a bit wider operating band and to match to the 50-ohm source impedance.

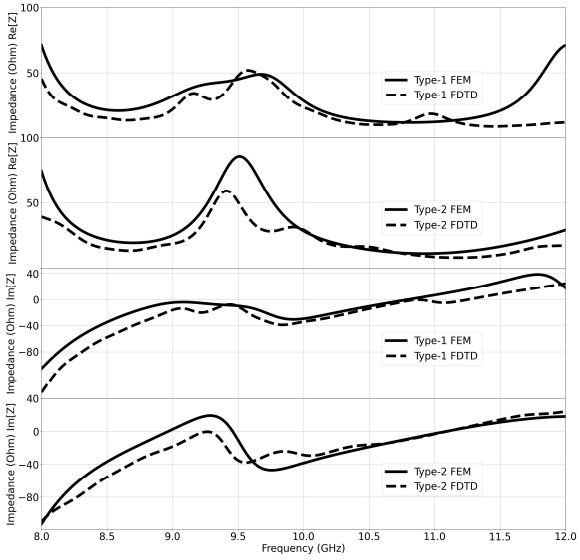

Figure 8. Response of input impedance consisting of real and imaginary components of the chessboard-coding planar antenna comparison between the FEM and FDTD approaches.

Figure 9 shows the reflection characteristic of the two design cases of chessboard alignment. The target responses coincide with an impedance response. In that, the frequency bandwidth occupies 8.9–9.8 GHz and 9–9.5 GHz with regard to the design antennas of the Type-1 and Type-2, respectively. The reflection dip level depends on impedance matching. These results are connected to the responses of the input impedance characteristic.

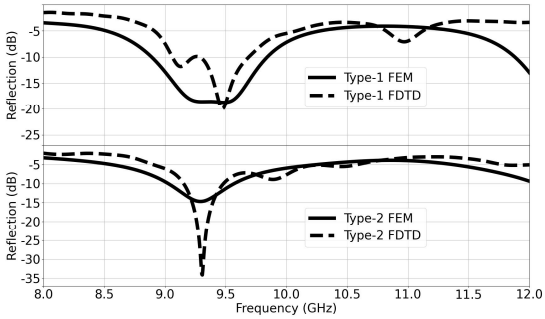

Figure 9. Response of reflection coefficient (S_{11}) of the chessboard-coding planar antenna comparison between the FEM and FDTD approaches.

Figure 10 and 11 show the radiation pattern of two chessboard-coding patterns of the Type-1 and Type-2 designs in an E-plane (x-z) and H-plane (y-z), respectively. Both design cases are depicted to the directional patterns. It is observed that a good main lobe beam belonging to the Type-2 design is better. The null response in the radiation pattern at ±90° theta angle is obtained and the gain at the boresight direction (0°) is enhanced. The resultant peak of the Type-1 design is 3.7 dBi, whereas the Type-2 design is 5.0 dBi. The improvement of radiation can be obviously evident by the reduction of the field scattering at the side radiation. Therefore, the scattering radiation is manipulated by a specific pattern employing the chessboard-coding surface in the Type-2 design.

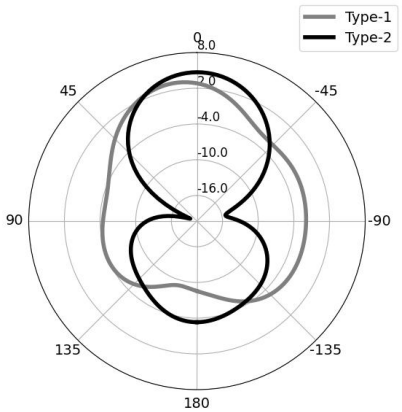

Figure 10. Response of E-plane radiation pattern of the chessboard-coding planar antenna.

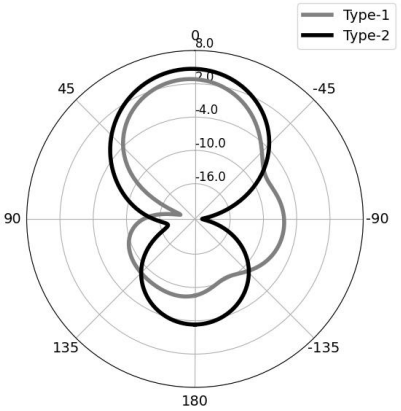

Figure 11. Response of H-plane radiation pattern of the chessboard-coding planar antenna.

3.3 The EM Field Distribution

The EM distribution is simulated using a finite element method (FEM) to understand a field configuration of the chessboard-coding artificial structures and planar antenna objects at 9.5 GHz. Firstly, the two models of the chessboard supercell are selected to observe the field profile. Secondly, the two designed types of planar antenna objects are also simulated to investigate the field patterns.

A. Supercell

Figure 12 and 13 show the graphic plot of the electric and magnetic field of the high-impedance surface and resonant cavity model. It is seen that the strong EM field effect occurs on the top layer, in that the reflection and transmission properties interact with the ground-backed and two-identical-layer structures, respectively. The strong electric field acts on the "0" elements (partially metallic patch) due to the oscillation depending on the operating wavelength. The magnetic field appears at the center of the supercell which is a joined contact in the alignment of the chessboard pattern. It reveals that the EM interaction between the four elements is coupling in terms of chessboard-coding cooperation. Hence, the numerical analysis of both models corresponds to providing an EM field configuration. With the unit-cell simulation, the excited field is a plane-wave characteristic, and these simulated models are realized as an infinitive supercell.

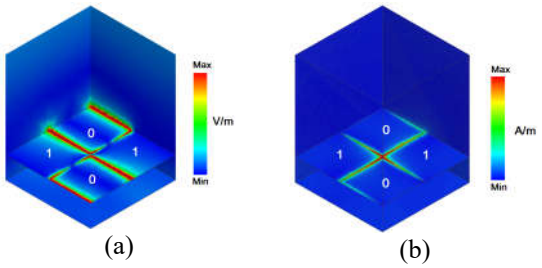

(a) (b)

Figure 12. Profile of a) electric (E) and b) magnetic (H) field distribution of supercell using the high-impedance surface model.

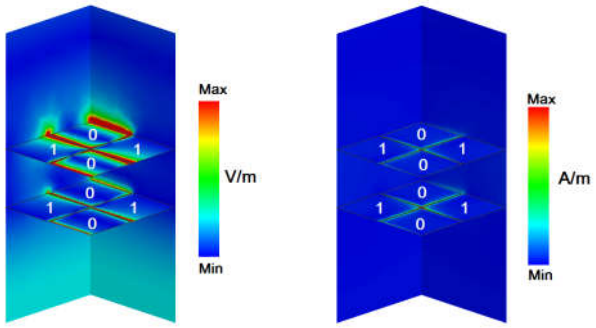

(a) (b)

Figure 13. Profile of a) electric (E) and b) magnetic (H) field distribution of the supercell using the resonant cavity model.

B. 5×5 Chessboard surface

Figure 14 shows the graphic plot of the electric field of both the proposed Type-1 and Type-2 planar antenna objects. Based on a setup environment of simulation, the excited field is from the narrow aperture element positioned close to the chessboard-coding surface by 2.0 mm. The field interaction is based on a near-field region and the parabolic wavefront is also taken into account. It results in the profile of the electric field effect that occurs on the chessboard surface symmetric along the electric-field excitation. (y-axis) With the good radiation pattern on the Type-2 designed pattern, the strong coupling effect occurs on the "1" elements. The concern in this EM activity is emphasized on a non-uniform wavefront fed by a close location of the narrow aperture.

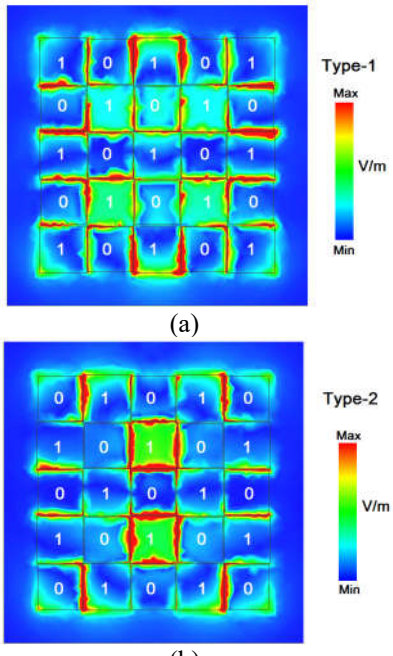

(a)

(b)

Figure 14. Profile of electric (E) field distribution of the chessboard-coding planar antenna: a) the Type-1 and b) the Type-2 design.

4. Conclusion

The characterization of the binary coding artifacts and the chessboard surface-based planar antenna objects have been demonstrated utilizing a numerical simulation based on a finite element method (FEM) and a finite-difference time-domain (FDTD) approach. The 2D chessboard-coding artificial structure is studied to illustrate the potential resonance effect of characteristics of reflection and transmission around the targeted frequency of 10 GHz. The binary-phase coding artifacts are formed by applying two kinds of phase-opposite unit cells consisting of the reflection phases of 0° and 180° as represented as the binary "0" and "1" elements. It can be built by using PEC and AMC structures which are based on a double-side dielectric slab configuration. It is shown that the designed supercell structures are studied in terms of the pattern evolution in order to understand the EM capability. The synthesis of the antenna objects is obtained to enhance the reduction of the scatting effect. This work contributes to the digital-based artifact formation using a 1-bit coding sequence leading to the development of complex coding patterns for intelligent wave objects in a next-generation wireless system.

References

[1] C. Della Giovampaola, N. Engheta, "Digital metamaterials", *Nature Mater*, vol. 13, pp. 1115–1121, 2014.

[2] T.J. Cui, M. Q. Qi, X. Wan, J. Zhao and Q. Cheng, "Coding metamaterials digital metamaterials and programmable metamaterials", *Light Sci. Appl.*, vol. 3, no. 10, pp. e218, October 2014.

[3] T. J. Cui et al., "Information metamaterial systems", *iScience*. vol. 23, no. 8, pp. 101403, 2020.

[4] S. Abadal, T.J. Cui, T. Low and J. Georgiou, "Programmable metamaterials for software-defined electromagnetic control: Circuits, systems, and architectures," *IEEE J. Emerg. Sel*., vol. 10, no. 1, pp. 6-19, March 2020.

[5] T. J. Cui, S. Liu, L.L. Li, "Information entropy of coding metasurface," *Light Sci Appl*, vol. 5, pp.e16172, 2016.

[6] N. Yu, P. Genevet, M. A. Kats, F. Aieta, J.-P. Tetienne, F. Capasso, et al., "Light propagation with phase discontinuities: Generalized laws of reflection and refraction", *Science*, vol. 334, no. 6054, pp. 333-337, October 2011.

[7] X. Luo, "Principles of electromagnetic waves in metasurfaces" *Sci. China: Phys. Mech. Astron*., vol. 58, pp. 594201, 2015.

[8] Q. Zhang, C. Liu, X. Wan, L. Zhang, S. Liu, Y. Yang, T.J. Cui, "Machine-learning designs of anisotropic digital coding metasurfaces," *Adv. Theory Simul.* vol. 2, pp.1800132, 2019.

[9] L. Li, H. Zhao, C. Liu, et al. "Intelligent metasurfaces: control, communication and computing," *eLight,* vol. 2, no,7, 2022.

[10] M. Paquay, J. -C. Iriarte, I. Ederra, R. Gonzalo and P. de Maagt, "Thin AMC Structure for Radar Cross-Section Reduction *IEEE Trans. Antennas Propag*, vol. 55, no. 12, pp. 3630-3638, Dec. 2007.

[11] J. C. Iriarte Galarregui, A. Tellechea Pereda, J. L. M. de Falcón, I. Ederra, R. Gonzalo and P. de Maagt, "Broadband radar cross-section reduction using AMC technology," *IEEE Trans. Antennas Propag.*, vol. 61, no. 12, pp. 6136-6143, Dec. 2013.

[12] J. Xue, W. Jiang and S. Gong, "Chessboard AMC surface based on quasi-fractal structure for wideband RCS reduction," *IEEE Antennas Wirel. Propag. Lett*., vol. 17, no. 2, pp. 201-204, Feb. 2018.

[13] H.P. Li, G.M. Wang, T. Cai, J. G. Liang and X.J. Gao, "Phase- and amplitude-control metasurfaces for antenna main-lobe and sidelobe Manipulations," *IEEE Trans. Antennas Propag*., vol. 66, no. 10, pp. 5121-5129, October 2018.

[14] Y. Zheng, J. Gao, X. Cao, Z. Yuan and H. Yang, "Wideband RCS reduction of a microstrip antenna using artificial magnetic conductor structures," *IEEE Antennas Wirel. Propag. Lett*., vol. 14, pp. 1582-1585, 2015.

[15] L. Zhang et al., "Realization of low scattering for a high-gain Fabry–Perot antenna using coding metasurface", *IEEE Trans. Antennas Propag*., vol. 65, no. 7, pp. 3374-3383, July 2017.

[16] Y. Zheng et al., "Wideband gain enhancement and RCS reduction of Fabry–Perot resonator antenna with chessboard arranged metamaterial superstrate", *IEEE Trans. Antennas Propag.,* vol. 66, no. 2, pp. 590-599, February 2018.

[17] A. P. Feresidis, G. Goussetis, Shenhong Wang and J. C. Vardaxoglou, "Artificial magnetic conductor surfaces and their application to low-profile high-gain planar antennas," *IEEE Trans. Antennas Propag*., vol. 53, no. 1, pp. 209-215, Jan. 2005.

[18] D. Breda, D. Liessi, "Floquet theory and stability of periodic solutions of renewal equations," *J Dyn Diff Equat*., 33, pp. 677–714, 2021.

[19] C. A. Balanis, *Babinet's Principle in Antenna Theory: Analysis and Design, 3rd ed*., Hoboken, NewYork, USA, John Wiley & Sons, Inc., pp. 616–620, 2005.

[20] R. N. Simons, *Coplanar Waveguide Short Circuit, in Coplanar Waveguide Circuits, Components and Systems, 1st ed*., New York, USA, Wiley-Interscience, pp. 241–243, 2001.

[21] B. A. Munk, *Element Types: A Comparison, in Frequency Selective Surfaces: Theory and Design, 1st ed*., New York, USA: Wiley-Interscience Publication, pp. 26–62, 2000.